

Fatigue studies on aluminum 6061/SiC reinforcement metal matrix composites

Fatigue is a process of progressive localized plastic deformation occurring in a material subjected to cyclic stresses and strains at high stress concentration locations that may culminate in cracks or complete fracture after a sufficient number of fluctuations. Fatigue testing is carried out using the ASTM D3479 with a notch or crack for investigating the initiation of crack. Several fatigue tests were conducted in tension-tension and/or tension-compression loading at a frequency of 10Hz or sinusoidal wave's frequency of 5Hz, and at constant-amplitude. The fatigue tests were interrupted by the researchers at regular intervals after a predetermined number of cycles to monitor crack advance and to observe the failure modes by various ways such as visual observation, digital camera, traveling microscope, CCD camera, etc.

Keywords: Fatigue, forging, wohler curves, silicon carbide, reinforcement.

1.0 Introduction

The initiation and subsequent propagation of cracks in a material due to cyclic loading is termed as fatigue. It begins with the initiation of a crack and grows progressively by small amounts with each loading cycle, typically producing striations on some parts of the fracture surface. The crack continues to propagate until it reaches a critical size, which is the point at which the stress intensity factor of the crack exceeds the fracture toughness of the material. This, therefore produces rapid propagation and then ultimately leads to complete fracture of the structure [1].

Conventionally the term fatigue was used interchangeably with metal fatigue, i.e., failure of metal components. In the nineteenth century, the sudden failing of metal railway axles was thought to be caused by the metal crystallizing because of the brittle appearance of the fracture surface, but this has since been disproved. Most materials seem to experience some sort of fatigue-related failure such as composites,

plastics and ceramics.

Fatigue tests are carried out to predict the fatigue life of a given component. Coupons are used to measure the rate of crack growth by applying cyclic loading at constant amplitude and averaging the measured growth of a crack over thousands of cycles. However, in special cases, the rate of crack growth may be found to be significantly different compared to that obtained from constant amplitude testing. One such case would be the reduced rate of growth that occurs for small loads near the threshold or after the application of an overload; and the increased rate of crack growth associated with short cracks or after the application of an underload.

If the loads are above a certain threshold, microscopic cracks begin to initiate at stress concentration zones such as holes; persistent slip bands (PSBs), composite interfaces or grain boundaries in metals. The stress values that cause fatigue damage are typically much lesser than the material's yield strength.

2.0 Fatigue studies – rotating fatigue testing machine

Experiments were conducted using a rotating-beam fatigue testing machine as shown in Fig.1. The governing principle behind the rotating-beam fatigue-testing machine is the technical theory of bending. This principle is based on the cantilever loading elastic beam bending principle [2]. A relatively long member that supports loads perpendicular to its axis is termed as a beam. Bending stress refers to the stress on a beam, on which applied moments tend to bend its layers.

The cantilever loading type of rotating bending fatigue test is an adaptation of this theory. A round specimen is subjected to a known constant bending stress (due to a bending moment) on the free end, while the other extreme end of the specimen is fixed, combined with the rotation of the sample-around the bending stress axis until failure occurs. The rotation and instantaneous bending on which the fatigue machine operates ensure that the bending stresses that lead to stretching of the upper layers of the specimen and compress the bottom layers are applicable in stationary beams, for which it should be evenly distributed around the entire circumference of the specimen. The stress-test is carried

Dr. Prashant S Humnabad, Dr. Hanamantraygouda M B, Assistant Professor and Prof. S B Halesh, Associate Professor, Department of Mechanical Engineering, Sir MVIT, Bengaluru, India. E-mail: hanumanthrayagowda_mech@sirmvit.edu /prashantsh_mech@sirmvit.edu / halesh_mech@sirmvit.edu

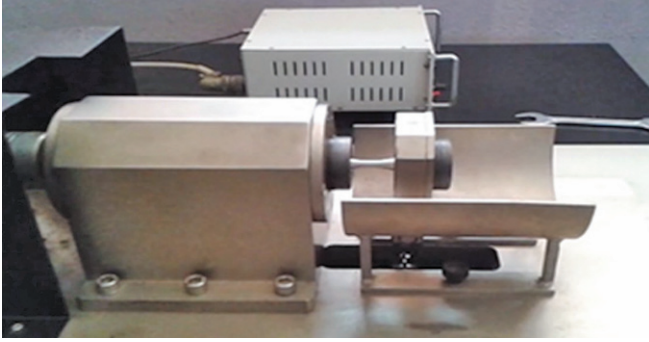


Fig.1: Rotating beam fatigue testing machine



Fig.2. Fractured fatigue specimen's

out by selecting a percentage (%) of the tensile strength of the test material and converting that value into a bending moment [3].

Once the specimen is mounted onto the machine collets, the machine is brought up to the desired speed by adjusting the speed control. The poise weight is then positioned on the calibrated beam to the bending moment previously calculated and locked into place. The machine automatically stops when the specimen fractures and the number is recorded from the cycle counter (digital indicator up to 9,99,999). The applied radial load is measured using a the load cell connected between the specimen holder and the loading lever. Below the bearing support, a part catcher is fixed to collect the specimen after fracture. Specimens tested at various loads provide data for plotting a stress versus number of cycles (S/N) curve. Fig.2 shows the specimen mounted on the collect.

3.0 Fatigue properties

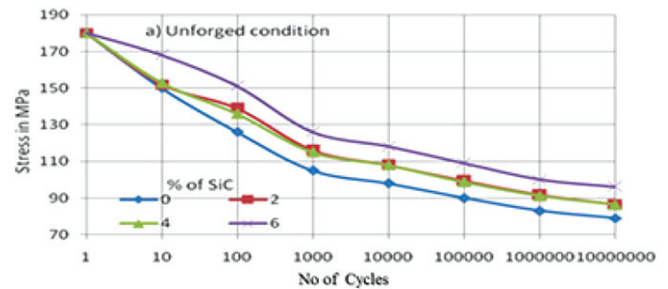
Fatigue tests were carried out in load control with a hydraulic test machine. A comparison of the stress versus strain cycles to failure behaviour of the unforged, 20%, 40% and 60% forged specimens for both matrix and the composites is given in Table 1 and Fig.3 shows how an increase in the content of SiC resulted in enhanced fatigue resistance of the composites independent of orientation. The magnitude of enhancement

of fatigue resistance is higher at lower wt% of SiC (0–2 wt%); however, no significant change can be seen at higher percentages (4 and 6 wt%). Several studies have shown that increasing the wt% of MMC particles enhanced the fatigue strength [4].

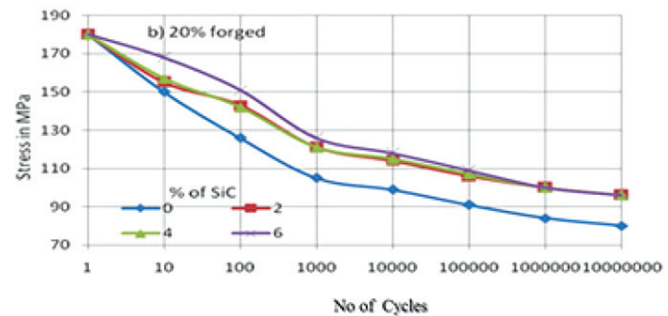
SiC particulates can bear the maximum fatigue load. The fatigue life of SiC-Al MMCs is usually longer than that of as-cast condition materials. The enhancement is due to the higher strength of SiC than the matrix materials.

The change in fatigue resistance versus forging condition is shown in Fig.4 for the matrix alloy and MMC specimens. The fatigue signature show that both forged and un-forged specimens showed a similar behaviour with the number of cycles.

The fatigue strength in the forged-condition specimen (20%, 40% and 60% forged conditions) shows that there is no significant change in the matrix alloy, but in the 2% SiC-reinforced MMCs, there are significant changes in their behaviours, as shown in Fig.5. On the contrary, there is no significant effect of forging on the fatigue resistance of the 4% and 6% reinforcements. The enhancement of fatigue strength is due to the addition of higher-stiffness SiC particulates into the Al MMCs; they help to load the transfer capacity of the interface. Sometimes, the elastic modulus reduces due to porosity and micro or macro cracks. It can also be confirmed that deformation contributes to the reduction of the elastic modulus in the presence of porosity. Forging reduces porosity to a great extent and this in-turn enhances mechanical strength as well as elastic modulus [5].



(a)



(b)

Fig.3: (a) Wo'ehler curves for Al and Al/SiC MMCs for (a) unforged and (b) 20% forged conditions

TABLE I. DATA SHOWING THE STRESS VALUES (MPa) AS A FUNCTION OF THE NUMBER OF CYCLES FOR Al AND AlSiC COMPOSITE AT DIFFERENT FORGING LEVELS

% SiC	Fatigue cycle							
	0	10 ¹	10 ²	10 ³	100 ⁴	10 ⁵	10 ⁶	10 ⁷
Unforged Condition								
0	180	150	126	105	98	90	83	79
2	180	152	139	116	108	99.5	91.7	86.3
4	180	153	136	115	108	98.8	91.1	86.3
6	180	168	151	126	118	109	100	96.1
20% forged								
0	180	150	126	105	99	91	84	80
2	180	155	143	121	114	106	100	96
4	180	157	142	121	115	107	100	96
6	180	168	151	126	118	109	100	96
40% forged								
0	180	155	132	111	104	96	89	86
2	180	156	144	122	115	106	101	96
4	180	159	144	122	116	107	101	98
6	180	170	153	127	120	111	102	97
60% forged								
0	180	152	128	107	100	92	85	82
2	180	154	142	120	112	104	98	93
4	180	156	141	119	113	104	97	93
6	180	169	152	126	119	110	101	96

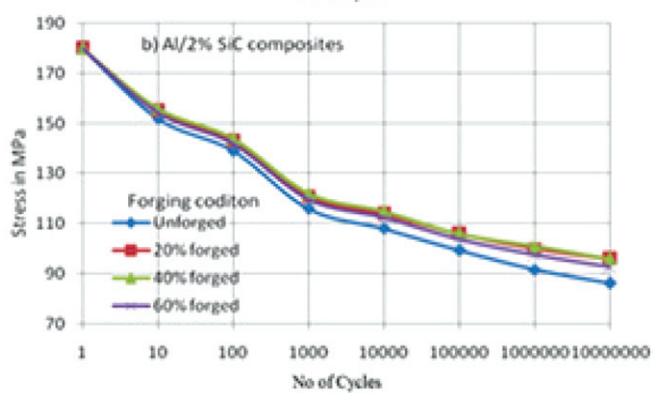
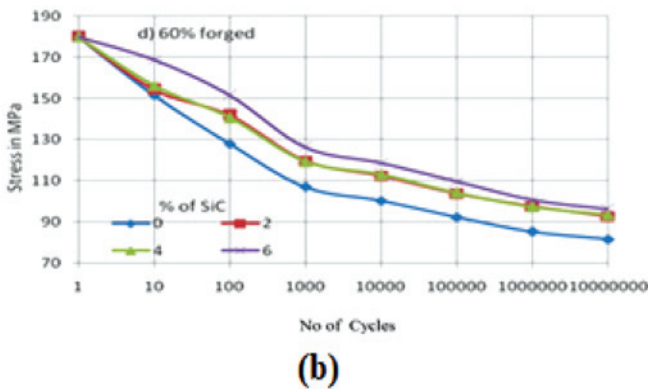
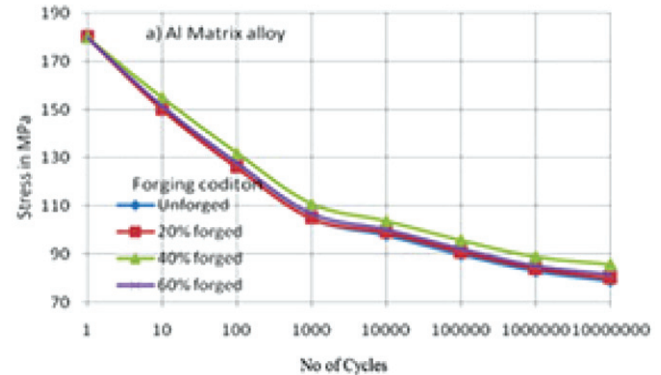
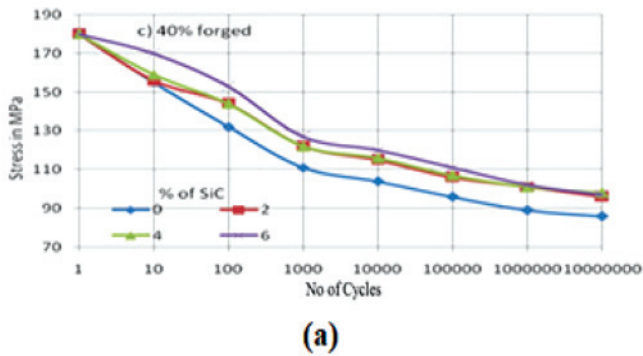


Fig.4: Wöhler curves for Al and Al/SiC MMCs for (c) 40% and (d) 60% forged conditions

Fig.5: Wöhler curves for (a) Al and (b) Al-2% SiC MMCs for different forged conditions

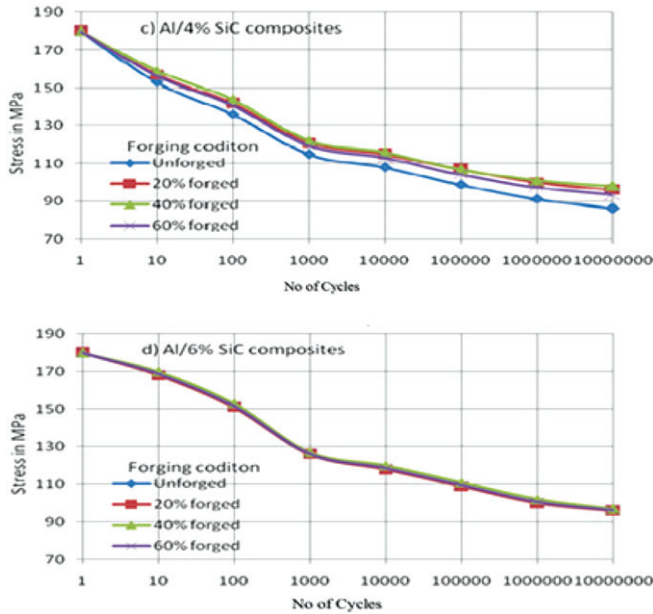


Fig.6: Woöhler curves for (c) Al/4% SiC and (d) Al/6% SiC MMCs for different forged conditions

4.0 Fatigue fracture studies

Typical fractured surfaces of matrix and Al-2 wt% SiC after fatigue fracture are shown in Fig.6(a) and (b) and Fig.6(c) and (d), respectively. From Fig.6(a), it can be seen that once crack initiation takes place at the pores two dissimilar fracture morphologies were observed, which marked the same ‘A’ (ductile fracture) and ‘B’ (brittle fracture), and fatigue crack (FC) propagated between these two regions. Region ‘A’ dominates more than region ‘B’, and fatigue cracks develop in the severely damaged region. Fig.6(b) shows the fracture surfaces of both stages of forging [6]. Al alloy, after fatigue failure, contains two regions ‘A’ (ductile failure) and ‘B’ (brittle failure). Region B dominates more than region ‘A’, which is because forging reduces the porosity and refines the grain boundaries of the matrix alloy. Similar to the unforged specimen, the crack (C) and FC are continuous and are formed in the severely damaged region Fig.6 show the fracture surface of the as-cast and forged conditions of Al-6wt% SiC particle-reinforced composites specimens, respectively. Unlike the Al matrix alloy, they do not show any two clear distinct regions in both as-cast and forged conditions [8]. Cavaliere noted that as the interspacing decreased, the degree of control due to triaxiality of stress increased, so striation formation was hindered and the dominant damage mechanism changed to void formation. After stable crack propagation, a fast fracture region was typically observed [9].

The large-scale fracture can be attributed to the high crack velocity associated with this portion of the fracture surface. The fracture surfaces also displayed the presence of very few cracks (Fig.6-b), probably originating from casting defects or during cooling in the fabrication process. This is in agreement with the increased density of the composite after forging [10]. The

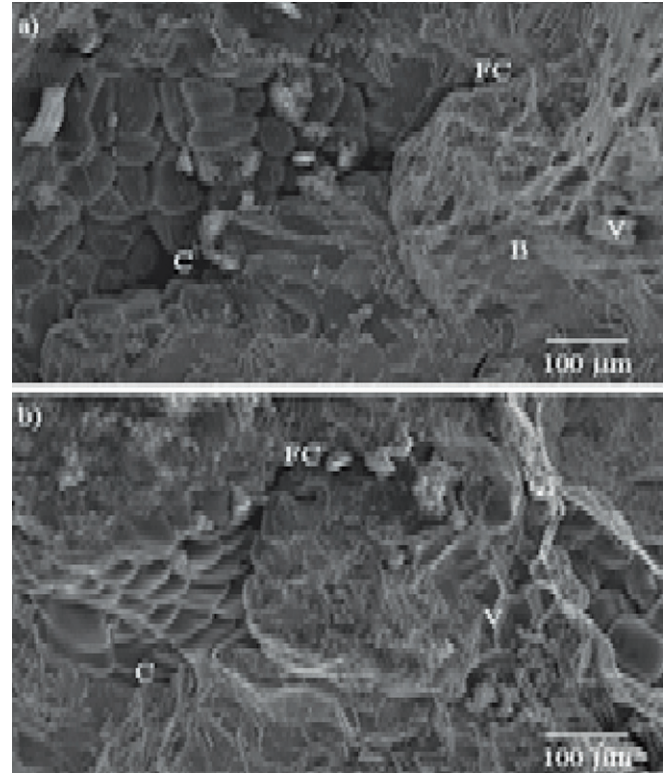


Fig.7: (a-b): Fracture surface of (a) unforged and (b) forged alloy specimen after fatigue failure. A-ductile fracture; B-brittle fracture; FC-fatigue crack; V-void in matrix

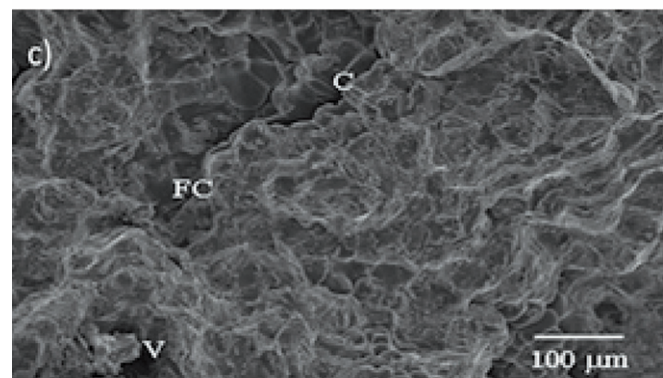
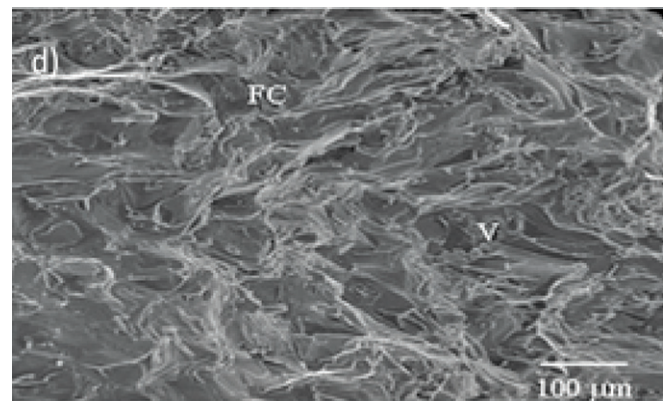


Fig. 8(a-b): Fracture surface of (c) unforged and (d) forged Al-6% SiC composite specimens

reduction in porosity causes the increase of ductility in the composites and this further leads to large elongated dimples, tear ridges and shear bands, which appear on the fracture surface. In the present work, the effects of SiC content and the forging process on the fatigue properties of Al/SiC MMCs are studied, and the following conclusions are drawn from the experimental observations. The microstructures of the as-cast and forged Al/SiC MMCs exhibit uniform distribution of SiC, and the porosity in the forged specimen substantially reduces [11]. The matrix alloy and MMCs behave more like monolithic materials because the homogeneous spatial distribution of the SiC enables efficient load transfer from the matrix to the reinforcement particle without producing stress concentration sufficient to initiate fatigue cracks. With increasing SiC content, the values of fatigue increased up to 4%, after which it decreased. Both forging of 20% and 40% stages increased the fatigue value for 2 wt% and 4 wt% SiC-reinforced MMCs, but had less-significant effect on other materials. SEM analyses of the fracture surfaces showed broken particles, surrounded by a ductile region and de-cohesion at the matrix and particulate interfaces. The tear ridges in the MMCs can be explained by the high local plastic constraints induced by a particle cluster [12].

5.0 Conclusions

Cold forging of an Al6061wt% SiC composite was tested at room temperature (25°C). This flow stress-strain curve is obtained from the cold forging experiment. The stress-strain curve data are uploaded in the Deform-3D software for FEA analysis. Furthermore, the microstructure characterization of Al-SiC material by using optical and SEM techniques is also studied. By using the Deform-3D FE tool, cold forging of Al-SiC composites was performed to evaluate the damage, velocity, and effective stress-strain distributions at different points of the trial. From the studies carried out, it can be concluded that:

- Al6061-SiC composites were successfully cold forged with height reduction of 35–40% without fracture. The damage in the billets were observed after 40–50% decrease in height and extreme damage occurs at 60%.
- Higher degrees of forging also affects mechanical properties, wear fatigue and corrosion properties of Al/SiC particles.
- Al-SiC with 6% SiC reinforcement possesses higher effective stress formation in all 12 cases studied with a value of 273 MPa in Deform.
- Analysis of forging of composite was performed using Deform-3D, and the distribution of effective stress, effective strain, effective strain rate, and velocity vector profile was determined. Higher magnitudes of effective stress and strain were found at the corners and edges of the billet. This was also confirmed by the presence of severe cracks at those regions during the present experimental investigations.
- The trend of increasing wear rate with the increase in wear

track distance in a linear fashion is obtained from the wear results. In forged conditions, the wear rate is found to be lower as opposed to higher wear rate in unforged conditions. The wear steadily increases with increasing sliding speed with the exception of sliding speed of 700 rpm, where it shows a lower wear rate. This is owing to the fact that the time taken to cover the sliding distance is lesser at higher speeds than that at lower speeds, considering constant sliding distance.

6.0 References

- [1] Piramanayagam, Sethu Ramalingam, Prabhakar M., Mayandi K., C.S Mahalakshmi, G Manigandan, P Mouleeshwaran and Kanna S.K. Rajesh (2020): Developing a Rotating Fatigue Test Machine and Testing with Dissimilar Materials. *Journal of Advanced Research in Dynamical and Control Systems*. 12. 631-638. 10.5373/JARDCS/V12SP5/20201798.
- [2] Jones D. (1987): Fatigue test machine. Patent Application Department of the Air Force, Washington, DC..
- [3] Macek Wojciech, Zawielak Stanisław, Deptuś Adam and Ulewicz Robert. (2019): Fatigue Testing Machines and Apparatus. *Quality Production Improvement*. 10. 80-108. 10.30657/qpi.2019.10.08.
- [4] Meggiolaro Marco, Castro Jaime and Nogueira Rodrigo. (2017): A Fast Rotating Bending Fatigue Test Machine. 10.26678/ABCM.COBEM2017.COB17-1824.
- [5] Macek Wojciech, Zawielak Stanisław, Deptuś Adam and Ulewicz Robert. (2019): Fatigue Testing Machines and Apparatus. *Quality Production Improvement*. 10. 80-108. 10.30657/qpi.2019.10.08.
- [6] IJIMA Noriko, Honma Shinya, Ryotaro Nakano, Hayashi Shota, Hirano Tomoki, Iijima Toshihiko and Yajima Yasutomo (2021): Fatigue properties of hollow zirconia implants. *Dental Materials Journal*. 40. 10.4012/dmj.2020-248.
- [7] Peng Zi, Sheng Jun, Wang Xu and Tang Yue. (2021): Low Cycle Fatigue Properties of FGH720Li Superalloy. *Materials Science Forum*. 1035. 292-296. 10.4028/www.scientific.net/MSF.1035.292.
- [8] Liu Chi, Ma Liyong, Zhang Ziyong, Fu Zhuo and Liu Lijuan. (2021): Research on the Corrosion Fatigue Property of 2524-T3 Aluminum Alloy. *Metals*. 11. 1754. 10.3390/met11111754.
- [9] Bai Yishan, Yang Shanglei, Zhu Minqi and Fan Cong. (2021): Study on Microstructure and Fatigue Properties of FGH96 Nickel-Based Superalloy. *Materials*. 14. 6298. 10.3390/ma14216298.
- [10] Lee J.H. and Cho Jaeung. (2017): A Fatigue Fracture Study on TDCB Aluminum Foam Specimen of Type Mode III Bonded with Adhesive. *Archives of Metallurgy and Materials*. 62. 10.1515/amm-2017-0208.
- [11] Hadzihafizovic Dzevad. (2021): *Fatigue fractures*. 10.13140/RG.2.2.11744.81929.
- [12] González-Velázquez Jorge. (2018):. *Fatigue Fracture*. 10.1007/978-3-319-76651-5_4.